Spectrochimica Acta Part A: Molecular and Biomolecular Spectroscopy 278 (2022) 121302

Contents lists available at ScienceDirect

Spectrochimica Acta Part A: Molecular and Biomolecular Spectroscopy

journal homepage: www.elsevier.com/locate/saa

Fluorescence study of the influence of centrifugation on graphene oxide dispersions in water and in tannic acid

Carlos Sainz-Urruela [a], Soledad Vera-López [a,b], Ana María Díez-Pascual [a,b], María Paz San Andrés [a,b,*]

[a] Universidad de Alcalá, Facultad de Ciencias, Departamento de Química Analítica, Química Física e Ingeniería Química, Ctra. Madrid-Barcelona Km. 33.6, 28805 Alcalá de Henares, Madrid, Spain
[b] Universidad de Alcalá, Instituto de Investigación Química Andrés M. del Río (IQAR), Ctra. Madrid-Barcelona Km. 33.6, 28805 Alcalá de Henares, Madrid, Spain

HIGHLIGHTS

- Tannic acid is a good natural bioactive dispersive agent for GO in water.
- Tannic acid and GO interact with riboflavin producing quenching simultaneously.
- Multiple regression is used to calculate the quenching constants with two quenchers.
- Centrifugation is a crucial step in the GO dispersion in water or tannic acid.

GRAPHICAL ABSTRACT

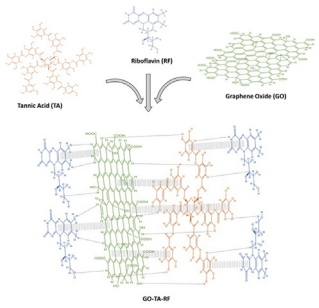

ARTICLE INFO

Article history:
Received 13 February 2022
Received in revised form 20 April 2022
Accepted 22 April 2022
Available online 28 April 2022

Keywords:
Graphene Oxide
Tannic Acid
Dispersion
Fluorescence
Centrifugation

ABSTRACT

Graphene oxide (GO) is acquiring a great interest in biomedicine, biotechnology and biochemistry due to its unique properties. However, GO layers are bound by van der Waals forces, which results in aggregation. An efficient dispersion of the aggregated nanostructures is crucial from an application viewpoint, hence eco-friendly procedures are pursued. In this work, the potential of tannic acid (TA) as a GO dispersant in water has been investigated for the first time. Transmission electronic microscopy (TEM) was used to visualize the degree of GO exfoliation in the dispersions. To further assess TA dispersant capability, a fluorescent biomolecule, riboflavin, has been selected. GO and TA cause a quenching effect on riboflavin fluorescence, which depends on the GO and TA concentration, the GO/TA weight ratio and the final centrifugation step that was found to be crucial. Multiple regression analysis has been used to determine the quenching constants for TA and GO simultaneously. The GO-riboflavin interaction weakens upon centrifugation. This step, traditionally used to remove the nanomaterial aggregates, should be avoided to obtain a high GO concentration in the dispersions. This study paves the way towards the use of environmentally friendly dispersant agents instead of conventional organic solvents or synthetic surfactants to attain high-quality dispersions of carbon nanomaterials in water.

© 2022 The Author(s). Published by Elsevier B.V. This is an open access article under the CC BY-NC-ND license (http://creativecommons.org/licenses/by-nc-nd/4.0/).

1. Introduction

Graphene (G), an atomically thick carbon monolayer obtained from the breakage of the Van der Waals forces of graphite, has recently gained a lot of interest in wide number of technological applications, owing to its unique electronic, thermal, optical, and mechanical properties [1,2]. Thus, it shows outstanding electrical

* Corresponding author at: Universidad de Alcalá, Facultad de Ciencias, Departamento de Química Analítica, Química Física e Ingeniería Química, Ctra. Madrid-Barcelona Km. 33.6, 28805 Alcalá de Henares, Madrid, Spain.
E-mail address: mpaz.sanandres@uah.es (M.P. San Andrés).

https://doi.org/10.1016/j.saa.2022.121302
1386-1425/© 2022 The Author(s). Published by Elsevier B.V.
This is an open access article under the CC BY-NC-ND license (http://creativecommons.org/licenses/by-nc-nd/4.0/).

and thermal conductivity [3], low density, very large surface area, optimal combination of high elasticity with high stiffness and strength [4], broad absorption spectral range, high optical transparency [5] and abundance, which make it very attractive material in various fields ranging from medicine or high-performance composites [6] to chemical sensors [7].

However, owed to its hydrophobic nature and strong van der Waals forces between adjacent sheets, G is insoluble in water and thus, difficult to be dispersed in common organic solvents, which hampers its applications. In this regard, graphene oxide (GO), an oxidized form of graphene comprising epoxide, hydroxyl and carbonyl groups on the basal planes and carboxylic acids on the edges [8], has been recently investigated in numerous works as an alternative to G. GO is a partially water-soluble nanomaterial; upon sonication in aqueous media, it easily exfoliates and forms stable colloidal suspensions due to its strong hydrophilicity [9]. Furthermore, it presents surface functionalization capacity and it is biocompatible [10]. GO can be synthesized by four main routes: Staudenmaier, Hofmann, Brodie, and Hummers. The most widely used is the Hummer's method in which $NaNO_3$, H_2SO_4 and $KMnO_4$ are used for the oxidation of graphite. However, novel methods have emerged to avoid the evolution of toxic gases and reduce the synthesis time. Electrochemical processes are highly desirable owed to their eco-friendliness, high efficiency, and inexpensiveness [11,12].

Bioactive compounds such as polyphenols, vitamins, carotenoids, omega-3 fatty acids, organic acids, nucleosides and nucleotides, and phytosterols have recently attracted countless attention due to their role in prevention of several chronic diseases [13]. Amongst the most common bioactive compounds found in our diets are polyphenols, which are well known for their antioxidant properties [14]. They inhibit or interfere with the process of free radical formation, preventing the oxidation of cells.. The simplest member of the group of hydrolysable tannins is tannic acid (penta-m-digallolyl glucose) (TA), $C_{76}H_{52}O_{46}$ [15], a water-soluble natural polyphenolic compound that comprises a large number of reactive functional groups such as hydroxyls (Fig. 1). It can be found in bananas, sorghum, wine, coffee, tea and beer [16], and exhibits antioxidant, antimutagenic, antiallergenic, anti-inflammatory, and anti-carcinogenic properties [17]. Besides, due to its chemical reactivity, bioactivity and biocompatibility, TA is a good candidate to obtain low-cost, environmentally friendly and scalable G dispersions in water. In this regard, TA has been used as a stabilizer to obtain G via exfoliation of graphite with ultrasounds, and the influence of several parameters such as TA concentration, pH, and sonication time were investigated [18].

Riboflavin, vitamin B_2, is a water-soluble vitamin present in some foods and available as a dietary supplement. This vitamin aids to keep healthy blood cells and to boost energy levels, prevents free radical damage, protects skin and eye health, and participates in the metabolism of other vitamins, fats, carbohydrates, and proteins. It is a naturally fluorescent molecule when it is exposed to UV light [19], with an excitation wavelength at 380 and 455 nm, and an emission wavelength at 520 nm. The molecular structure of riboflavin consists of a flavin ring component and four hydroxyl groups covalently bonded to an aliphatic chain that is attached to the flavin ring moiety, as shown in Fig. 1. Taking into account the huge nutritional value of this vitamin, it was chosen as a fluorescent probe in this study. The fluorescence intensity of riboflavin decreases in the presence of certain species, known as quenchers, that have the ability to interact with this molecule and reduce the emitted intensity via quenching effect [20–23].

Over recent years, a wide variety of ionic and non-ionic surfactants have been used to obtain stable dispersions of G and GO in aqueous media [24,25]. However, most of them are of synthetic origin, which raises concerns regarding cost, environmental impact, toxicity or biocompatibility of the resulting materials. Recently, different types of biomolecules including proteins/peptides, nucleotides / DNA, polysaccharides, bile salts, etc., have been used to produce biocompatible dispersions of G [26]. In a pioneering work, Laaksonen *et al.* [27] identified a special class of surface-active proteins involved in the growth and development of filamentous fungi, called hydrophobins, as highly suitable dispersants for exfoliation of graphite into G aqueous medium. More recently, phospholipids such as lecithin and phosphatidylcholine have been used as dispersing agents for G [28,29], and colloidal stabilization was achieved by adsorption of inverse micelles and hemimicelles of phospholipids on the graphitic basal plane, which prevent aggregation of the exfoliated G sheets by the entropic repulsion of the hydrophobic lipid chains. Bioactive molecules with antioxidant character such as *trans*-resveratrol [30] and other polyphenols such as coffee [31], green and black tea [32,33] have also been used

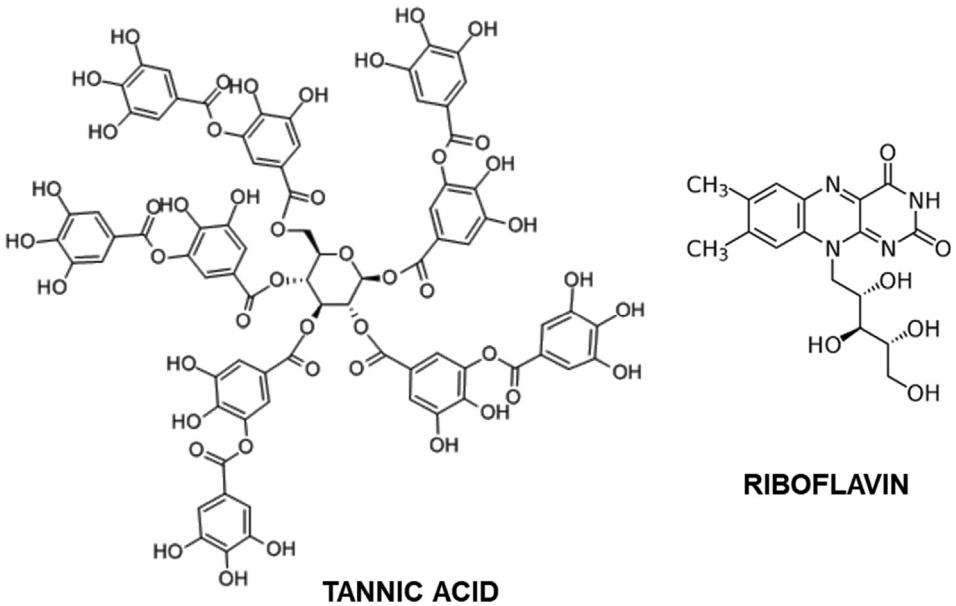

Fig. 1. Molecular representation of tannic acid (TA) and riboflavin.

for G exfoliation. The aforementioned studies demonstrate the great potential of biomolecules and bioactive compounds to produce stable dispersions of G by sonication in aqueous medium as an easy, economical and environmentally friendly way.

In this work, the efficiency of TA as a dispersant agent for GO in aqueous media has been assessed for the first time. The main aim is to use a biocompatible media and replace the conventional synthetic dispersing agents, in search of a more sustainable and greener process. To investigate the interactions between GO and TA, riboflavin has been selected as a fluorescent probe. Results show that GO dispersed in TA quenches riboflavin fluorescence, and the quenching magnitude depends on several factors including the GO and TA concentration as well as the GO/TA mass ratio. Besides, the use of a centrifugation stage for the dispersion of GO, which has not been previously assessed, has been found to be critical in the level of GO exfoliation attained.

2. Materials and methods

2.1. Reagents

Graphene oxide (GO, av-Gox-70) comprising sheets with an average thickness of 70 μm, was provided in powder form by Avanzare Innovación Tecnológica, SL (Logroño, Spain). Tannic acid (M_w: 1701.20 g mol^{-1}) was purchased from Sigma-Aldrich Corp. (St. Louis, Missouri, United States). Riboflavin ($C_{17}H_{20}N_4O_6$, M_w = 376.36 g/mol) and phosphoric acid (H_3PO_4) were provided by Sigma-Aldrich (Madrid, Spain). Sodium hydroxide (NaOH) was obtained from Panreac (Barcelona, Spain) and ultrapure water was obtained in a Milli-Q system from Millipore (Milford, USA). All the reagents were of analytical grade and used as received.

2.2. Instrumentation

Fluorescence spectra were recorded on a LS 50B fluorescence spectrometer (PerkinElmer, Waltham, Massachusetts, USA) at 25 ± 1 °C. The excitation and emission slits were set at 5 nm and the scan speed was set at 500 nm min^{-1}. Quartz cuvettes with 1-cm pathlength were used for the measurements.

GO dispersions were prepared with the aid of an Elmasonic S 30 ultrasonic bath (Elma Schmidbauer GmbH, Singen, Germany) and a UP400S ultrasound probe (Hielscher Ultrasonics, Teltow, Germany). A Digicen centrifuge (Orto Alresa, Madrid, Spain) was used to speed up the sedimentation process. pH measurements were performed with a WTW Inolab pH/ion Level 2 pH-meter (Inolab, México D.F.).

The morphology and degree of dispersion of GO in tannic acid (TA) was observed by transmission electron microscopy (TEM) measurements performed on a Zeiss EM-10C/CR microscope (Oberkochen, Germany) with a voltage of 60 kV.

Multiple regression analysis has been carried out using the Statgraphics Centurion XVII 17.0.16 software.

2.3. Procedure

2.3.1. Preparation of the solutions

TA solutions (500 and 2000 mg L^{-1}) in ultrapure water were prepared at pH 7.1. The pH was adjusted with a 0.01 M NaOH solution. A stock solution of riboflavin was prepared with 28% v/v H_3PO_4 and stored at 4 °C under dark conditions. Working solutions were prepared by dilution, and the riboflavin concentration for studying the interaction between TA and GO was 0.6 mg L^{-1}.

2.3.2. Preparation of GO dispersions in water and tannic acid

Dispersions were prepared in duplicate by weighing the necessary amount of GO and adding the required volume of ultrapure water or TA aqueous solution (500 and 2000 mg L^{-1}), up to a volume of 100 mL. The final GO concentrations obtained were 0, 10, 20, 30 and 40 mg L^{-1}. The samples were then sonicated in the ultrasonic bath for 30 min at a frequency of 37 kHz, and then exposed to the ultrasonic probe for 5 min at a frequency of 24 kHz to complete the dispersion. Finally, to study the influence of the centrifugation step on the GO dispersions, half of them were centrifuged leaving the rest without centrifugation. A schematic representation of the preparation process of GO dispersions in TA is shown in Scheme 1.

2.3.3. Riboflavin fluorescence spectra

The fluorescence spectra of riboflavin, 0.6 mg L^{-1}, were recorded as 3D contour graphs to choose the optimal excitation and emission wavelengths. Spectra were recorded in water, in the 500 and 2000 mg L^{-1} TA aqueous solutions, at a pH of 7.1, and in the presence of different GO/water and GO/TA dispersions. The initial excitation wavelength was set at 300 nm, and 25 spectra were registered with an increment of 10 nm.

3. Results and discussion

3.1. Effect of tannic acid concentration on the fluorescence of riboflavin.

The potential of TA as dispersing agent for graphene (G) has been previously studied [34]. In such work, an important decrease in the fluorescence of riboflavin was found due to a strong interaction between the molecules. This interaction was observed in ultrapure water (pH = 4.1, the pH of the TA aqueous solution) as well as in a solution at pH 7.1. However, no interaction was observed between riboflavin and G dispersed in TA at pH 4.1, while a marked decrease in riboflavin fluorescence was found for G dispersions at pH 7.1. At highly basic conditions, all the hydroxyl groups of TA are deprotonated, and the hydrogen bonding interactions between TA and riboflavin are weakened. In the light of these results, 7.1 was chosen as working pH in the present work. At this pH, the fluorescence spectrum of riboflavin shows two maxima excitation wavelengths (380 and 455 nm) and an emission wavelength of 520 nm. The emission spectra of riboflavin in water and in the presence of TA for an excitation wavelength of 455 nm are shown in Fig. 2**a**. Fig. 2**b** shows the fluorescence intensity ratio of riboflavin in TA aqueous solutions (F) and in water (F_0). A significant decrease in the fluorescence intensity of riboflavin is observed with increasing TA concentration, by up to 20% and 58% for TA 500 and 2000 mg L^{-1} solutions, respectively. Between the centrifuged and non-centrifuged solutions, hardly difference was found, as expected, since the TA is completely dissolved in the medium.

It is important to note that riboflavin, a hydrophilic molecule, interacts strongly with TA since the fluorescence is decreased via structure modification by H-bonding and π-π interactions between the isoalloxazine rings of the vitamin and the phenolic rings of TA, as depicted in Scheme 2. Previous studies investigated the nature of the interactions between TA and other biological molecules like hemoglobin, a hydrophobic molecule, by fluorescence spectroscopy. In such case, the Van der Waals forces and hydrophobic interactions predominate and are responsible for the quenching effect [35].

The decrease found in the fluorescence of riboflavin in the presence of TA fits the Stern-Volmer equation as it was previously demonstrated [34], although it is not possible to discriminate the type of quenching taking place by steady state fluorescence measurements. However, it is probable that the interactions described

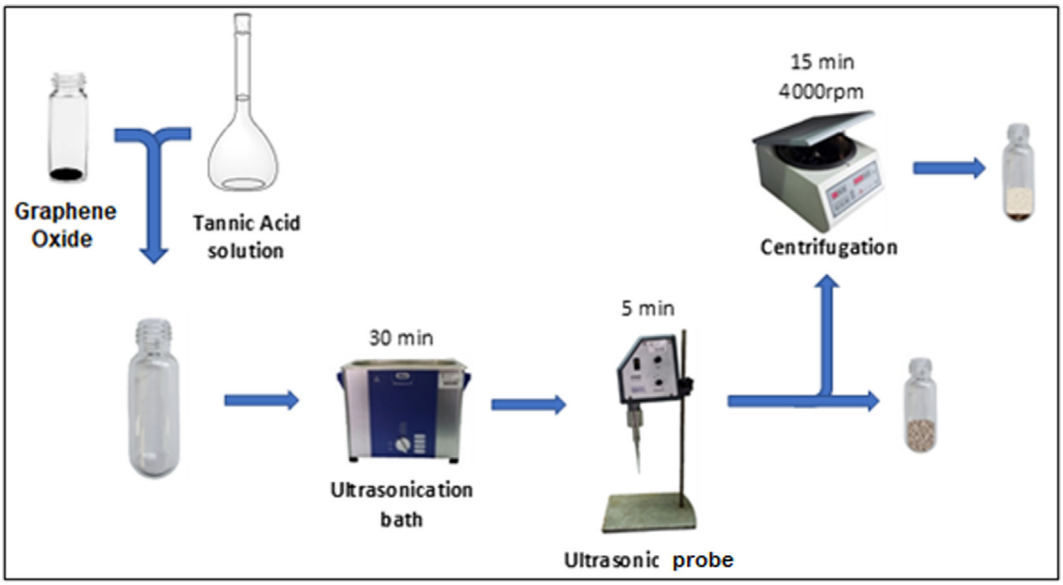

Scheme 1. Representation of the preparation process of GO dispersions in TA with and without centrifugation.

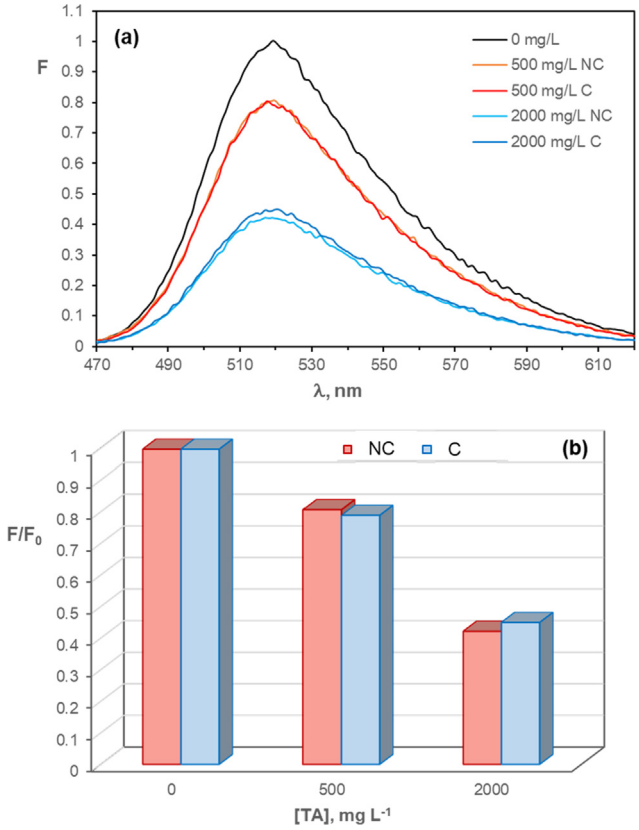

Fig. 2. Fluorescence spectra of riboflavin in water and in TA aqueous solutions (500 and 2000 mg L^{-1}) (a). Fluorescence intensity ratio (F/F_0) as a function of the TA concentration (b). Non-centrifuged (NC) and centrifuged (C). $\lambda_{exc}/\lambda_{em}$ = 455/520 nm. pH = 7.1.

above lead to a static quenching due to a supramolecular complex formation. The value calculated in our previous work for the quenching constant (K) at a pH of 7.1 was 0.00072 L mg^{-1} ($1.2x10^3$ M^{-1}), which will be compared with those determined in this study.

3.2. Fluorescence quenching of the fluorescence of riboflavin by graphene oxide in the absence of tannic acid.

3.2.1. Riboflavin fluorescence in the presence of graphene oxide dispersions in water.

Due to its polar functional groups, GO can be partially dispersed in water without the need for centrifugation. However, the centrifugation of the GO dispersions could promote the separation of the agglomerated sheets that may remain in the dispersion. The fluorescence of riboflavin 0.6 mg L^{-1} in the presence of GO dispersions in water (10, 20, 30 and 40 mg L^{-1}), without any dispersant, was tested for both non-centrifuged and centrifuged solutions. Fig. 3 shows the fluorescence spectra of riboflavin in the presence of GO dispersions with and without centrifugation and the decrease in the F/F_0 ratio produced by GO.

A very important decrease in riboflavin fluorescence is observed when GO is dispersed in the medium without centrifugation, Fig. 3**a**. In this case, given that there is no dispersant, the ultrasonic probe disperses the GO properly, and allows it to strongly interact with riboflavin, decreasing its fluorescence by 33, 46, 66 and 81% for GO concentrations of 10, 20, 30 and 40 mg L^{-1}, respectively, Fig. 3**b**. However, when the GO dispersions in water were centrifuged for 15 min at 4000 rpm, the nanomaterial settled to the bottom of the tube and almost nothing remained in the solution, leading to smaller decreases in riboflavin fluorescence, by about 5, 11, 16 and 26% for the abovementioned GO concentrations, respectively, Fig. 3**b**.

Therefore, in the absence of a dispersant, GO can be partially dispersed in water without centrifugation. After being subjected to the ultrasound probe, GO produces a decrease in the fluorescence of riboflavin by interaction in the bulk dispersion. Regarding the centrifuged dispersions, the concentration of GO in the bulk dispersion is much lower and therefore, less riboflavin-GO interaction occurs, hence the drop in the fluorescence of riboflavin is smaller than in the centrifuged dispersions.

3.2.2. Stern-Volmer relationship for riboflavin fluorescence in the presence of graphene oxide in absence of tannic acid

The Stern-Volmer relationship was applied to calculate the fluorescence quenching constants for initial GO dispersions with concentrations of 10 mg L^{-1}, 20 mg L^{-1}, 30 mg L^{-1} or 40 mg L^{-1}, diluted

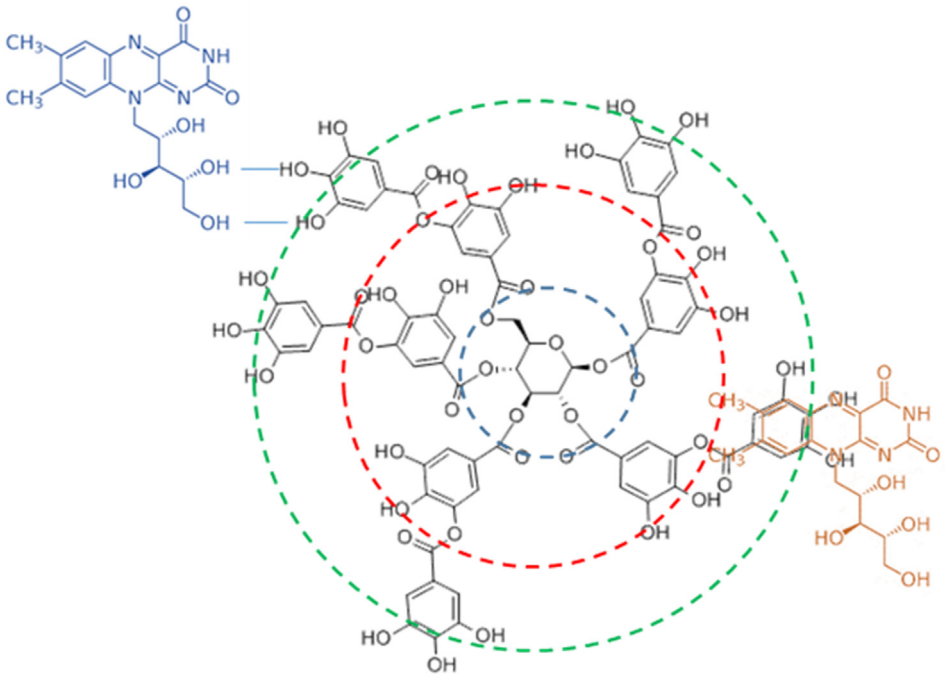

Scheme 2. Representation of the H-bonding and π-π interactions between riboflavin and TA.

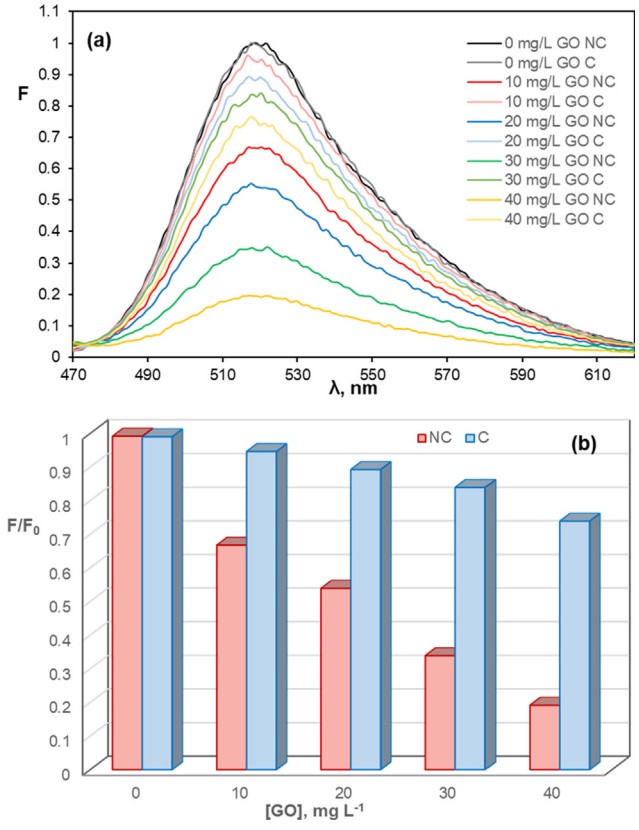

Fig. 3. Fluorescence spectra of riboflavin in water and in GO aqueous dispersions (10, 20, 30 and 40 mg L^{-1}) (a). Fluorescence intensity ratio (F/F_0) as a function of the GO concentration (b). Non-centrifuged (NC) and centrifuged (C). $\lambda_{exc}/\lambda_{em}$ = 455/520 nm. pH = 7.1.

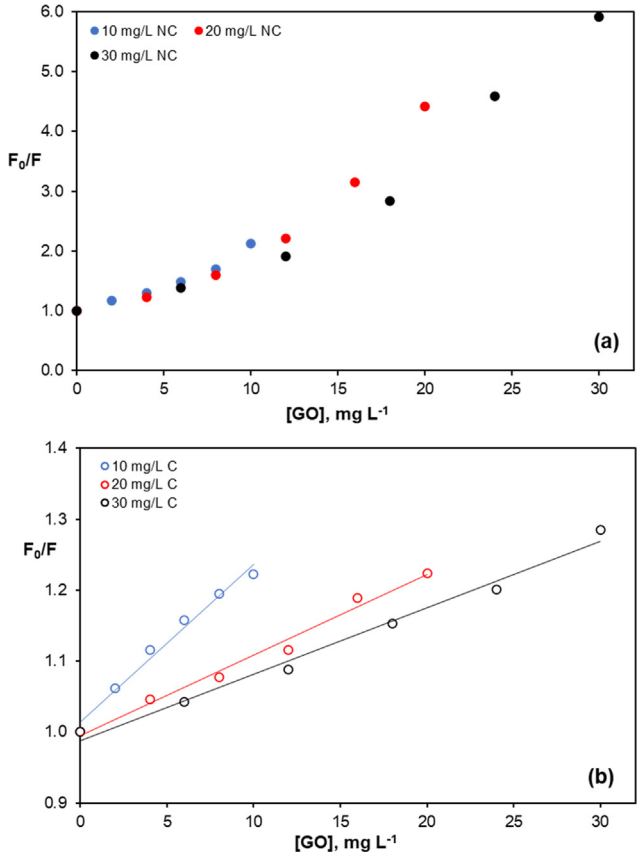

Fig. 4. Stern-Volmer plot for riboflavin 0.6 mg/L in the presence of GO aqueous dispersions without (a) and with centrifugation (b). $\lambda_{exc}/\lambda_{em}$ = 455/520 nm. pH = 7.1.

with water, although great variability was found amongst some measurements, likely because the GO was not homogeneously dispersed. The F_0/F ratio is plotted in Fig. 4**a** for dispersions without centrifugation. As can be observed, the relationship is exponential for the non-centrifuged ones, indicative of a combination of both dynamic and static quenching [21].

The values of F_0/F for the centrifuged dispersions are plotted in Fig. 4**b**. In such dispersions, most of the GO sinks to the bottom of the centrifugation tube, hence only a very small amount is dispersed, thus the change in the fluorescence of riboflavin with increasing GO concentration is very small, although the relationship between F_0/F and GO concentration is linear in the GO concentrations studied.

It is clear and highly important that the dispersion of GO in water can be achieved with the ultrasonic probe, but the subsequent centrifugation causes most of the sheets to fall to the bottom of the tube, which produces a new agglomeration, hence they cannot interact with riboflavin. Only a few GO sheets remain in the dispersion and are prone to interact with the vitamin.

In addition, the higher the GO concentration, the lower the slope of the Stern-Volmer plot. This is due to the centrifugation process that causes agglomeration of the GO sheets, leaving only a small amount in the bulk dispersion, and this effect becomes stronger with increasing GO concentration. Overall, the centrifugation of the GO dispersions does not result in an effective exfoliation of the GO sheets and causes the removal of most of the nanomaterial.

The quenching constants obtained from the Stern–Volmer plot for both centrifuged and no-centrifuged dispersions are collected in Table 1. As can be observed, in the centrifuged dispersions, K values decrease with increasing GO concentration, but the values are lower than those obtained for the non-centrifuged dispersions in their linear range at low concentrations.

The results mentioned above demonstrate that an effective dispersant is required to disperse GO in water, since, although it is partially soluble, aggregates formed by several sheets remain non-homogeneously suspended in the medium, as can be clearly observed in Fig. 5**a**. Upon centrifugation, the GO aggregates settle at the bottom of the tube, as shown in Fig. 5**b**. In this case, only a few sheets remain dispersed in the water medium.

3.3. Fluorescence of riboflavin in GO dispersions (0, 10, 20, 30 y 40 mg L-1) in tannic acid (500 and 2000 mg L^{-1}).

3.3.1. Riboflavin fluorescence in the presence of graphene oxide dispersion in tannic acid.

Tannic acid, a bioactive macromolecule that has a large number of hydroxyl groups, was used as dispersing agent for GO, since both compounds can interact strongly via different interactions, as discussed previously. The dispersions were prepared with two different TA concentrations (500 and 2000 mg L^{-1}) and different amounts of GO in order to obtain final GO concentrations of 10, 20, 30 and 40 mg L^{-1}. For dispersions in 2000 mg L^{-1} TA, the GO percentages were 0.5, 1.0, 1.5 and 2.0 wt%, while for dispersions in 500 mg L^{-1} TA, the percentages were 2.0, 4.0 and 6.0 and 8.0 wt%. The fluorescence of riboflavin decreases for both dispersions without and with centrifugation, indicating that the presence of TA promotes the nanomaterial exfoliation. Fig. 6 shows the fluorescence spectra and the decrease in intensity found at the maximum emission wavelength of riboflavin for the non-centrifuged dispersions. As mentioned previously, the fluorescence drops strongly in the presence of TA, and further decreases upon addition of GO, this decrease being an additional 14–17% every 10 mg L^{-1} of GO that is added to the dispersion. This decrease is very similar to that produced by GO in water in the absence of TA (13–16%) as the concentration of GO is increased by 10 mg L^{-1}.

A significant decrease in riboflavin fluorescence is observed for the GO (10 mg L^{-1}) in 500 mg L^{-1} and 2000 mg L^{-1} TA compared to the solution with the same TA concentration in the absence of nanomaterial. However, as the concentration of GO is subsequently increased, the drop in fluorescence intensity hardly changes, likely because it is not possible to effectively disperse more GO in the bulk solution.

Fig. 7 shows the fluorescence spectra and the decrease in intensity found in the maximum emission wavelength of riboflavin for centrifuged dispersions. The corresponding 3D fluorescence contour graphs showing the excitation and emission processes simultaneously are included in **Figure S1** in the supplementary material. As can be observed, the excitation spectra remain unchanged upon addition of GO to the medium, independently of its concentration (2000 or 500 mg L^{-1}). F/F_0 ratio for GO dispersions in TA with centrifugation is shown in Fig. 7**d**. In all cases, the diminution in the fluorescence intensity is very small, and much lower than that found for the non-centrifuged dispersions (Fig. 6).

Centrifugation is again a limiting step to obtain the final dispersion both in the absence of TA, as mentioned earlier, and in the presence of TA. Upon centrifugation, for any TA concentration, only a small amount of GO remains in the solution while a large quantity is removed in the residue. Likely, almost no interaction between riboflavin and GO takes place as GO concentration increases both in the absence and in the presence of TA, either 500 or 2000 mg L^{-1}. The presence of TA leads to an increased interaction between riboflavin and GO in the dispersions without centrifugation, but this physical operation reduces drastically the amount of GO dispersed in the medium.

3.3.2. Stern-Volmer relationship for riboflavin fluorescence in the presence of graphene oxide dispersions in tannic acid.

The plot of F_0/F ratio *vs.* GO concentration in the range of 0 to 40 mg L^{-1}, shows a non-linear trend for all the dispersions prepared (Fig. 8**)**. For non-centrifuged dispersions, as the concentration of TA in the medium increases, the quenching effect produced by GO is reduced. This could be explained considering that TA is the component that produces a stronger decrease in fluorescence, and in the presence of GO this quenching effect is attenuated, likely due to a competition between GO and TA to interact with riboflavin. In particular, for a GO concentration of 40 mg L^{-1}, a stronger decrease in riboflavin fluorescence is found for a TA concentration of 2000 mg L^{-1}.

The mechanisms of the quenching process (i.e., by both collisions and by complex formation with the fluorophore, respectively) seems to be a mixture of the dynamic and static processes. Indeed, when some fluorophore molecules form a complex with the quencher in the ground state, and the others transfer part of their energy to the quencher via collisions, the Stern-Volmer relation shows an exponential trend [21–23]. A linear relationship is only found at low concentrations (below 8 mg L^{-1} GO).

To get further insight into the quenching mechanism, fluorescence measurements in the temperature range between 25 and 35 ^{0}C were carried out. As an example, the excitation and emission spectra of riboflavin in the presence of 20 mg L^{-1} GO dispersed in

Table 1
Parameters obtained by fitting the experimental results to the Stern-Volmer equation regarding the fluorescence quenching produced by GO on riboflavin fluorescence (least-square fit procedure).

	[GO], mg L^{-1} (linear range, mg L^{-1})		
CENTRIFUGED	10 (0–10)	20 (0–20)	30 (0–30)
Intercept	1.01 ± 0.01	0.993 ± 0.007	0.994 ± 0.005
K, L mg^{-1}	0.022 ± 0.002	0.0112 ± 0.0005	0.0085 ± 0.0003
r	0.9918	0.9952	0.9979
NON– CENTRIFUGED	10 0 – 6	20 0 – 12	30 0 – 12
Intercept	1.00 ± 0.01	0.9 ± 0.1	0.98 ± 0.05
K, L mg^{-1}	0.080 ± 0.003	0.10 ± 0.01	0.076 ± 0.006
r	0.9986	0.9788	0.9965

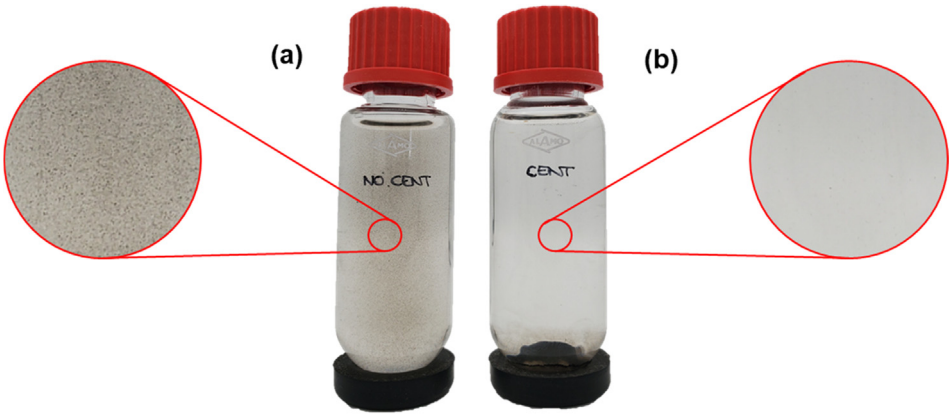

Fig. 5. Dispersion of 20 mg L^{-1} GO in water before (a) and after centrifugation (b).

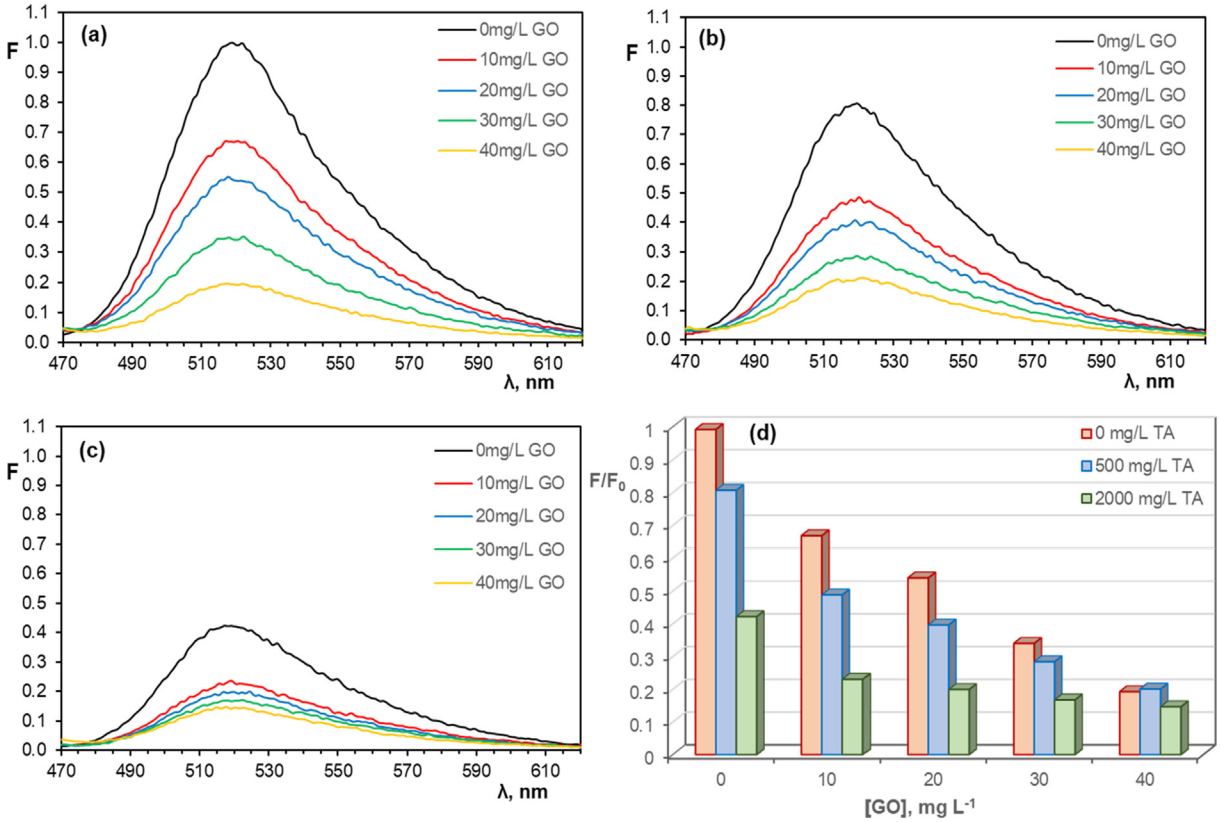

Fig. 6. Fluorescence spectra of riboflavin in 0, 10, 20, 30 and 40 mg L^{-1} GO for non-centrifuged dispersions in water, Section 3.2.1., (a); 500 mg L^{-1} TA (b) and 2000 mg L^{-1} TA (c). Fluorescence intensity ratio (F/F_0) as a function of GO concentration for the three media (d). $\lambda_{exc}/\lambda_{em}$ = 455/520 nm. pH = 7.1.

2000 mg L^{-1} TA are shown in **Figure S2** in the supplementary material. Similar behaviour was found for 40 mg L^{-1} GO dispersed in 2000 mg L^{-1} TA. Results suggest very small change in the fluorescence intensity values with increasing temperature, which is consistent with a static quenching mechanism [21]. Thus, although the two mechanisms can occur, the static quenching likely predominates.

Regarding the centrifuged dispersions, the decrease in fluorescence intensity is significantly smaller, and hardly depends on the GO concentration. In this case, the nanomaterial does not produce an additional quenching to that induced by TA. This corroborates that upon centrifugation, most of the GO falls to the bottom of the tube, hence it cannot interact with the vitamin dissolved in the medium. On the other hand, it was not possible to obtain good linear relationships between F_0/F ratio and GO concentration, hence the quenching constants have not been calculated.

In order to study the F_0/F ratio in the presence of both quenchers, GO and TA simultaneously, multiple regression analysis of the data was performed for both centrifuged and non-centrifuged dispersions, and the results are shown in Table 2. The relationship between the experimental F_0/F data and the corresponding values predicted by the theoretical model are shown in **Figure S3** in the supplementary material. F_0/F data fit well the linear equation with R^2 higher than 90% in both cases. The GO coefficient is significantly higher for non-centrifuged dispersions, indicative of a stronger interaction between riboflavin and GO. Conversely, in the case of TA, the coefficient is very similar for non-centrifuged and centrifuged dispersions, despite the amount of GO well-dispersed in

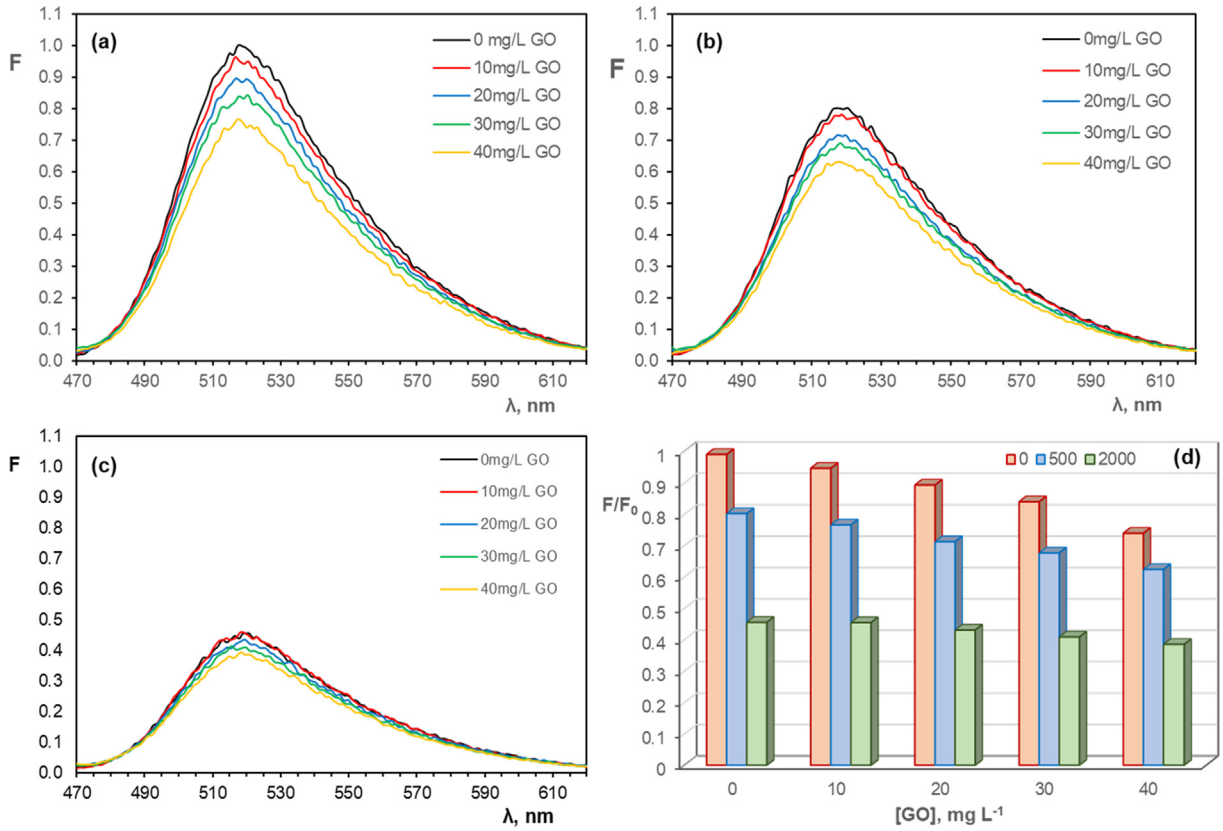

Fig. 7. Fluorescence spectra of riboflavin in 0, 10, 20, 30 and 40 mg L^{-1} GO for centrifuged dispersions in water, Section 3.2.1., (a); 500 mg L^{-1} TA (b) and 2000 mg L^{-1} TA (c). Fluorescence intensity ratio (F/F_0) as a function of GO concentration for the three media (d). $\lambda_{exc}/\lambda_{em}$ = 455/520 nm. pH = 7.1.

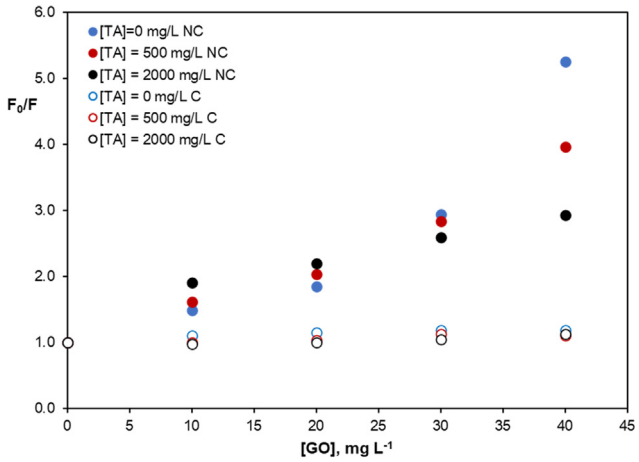

Fig. 8. Stern-Volmer plot for riboflavin 0.6 mg/L in the presence of GO dispersions in water, Section 3.2.1., 500 mg L^{-1} and 2000 mg L^{-1} TA solutions, non-centrifuged (NC) and centrifuged (C). $\lambda_{exc}/\lambda_{em}$ = 455/520 nm. pH = 7.1.

the TA medium decreases upon centrifugation, it seems that the interaction between riboflavin and GO does not depend on the TA concentration in the medium.

It is very important to note that the K value obtained for the quenching produced by TA in the absence of GO (K = 0.00072 L mg^{-1}) [34], is the same to those obtained in the multiple regression for TA (K_{TA}). This implies that the interaction between riboflavin and TA is the same in the absence and in the presence of GO, and that the differences in the presence of GO are due to the amount of GO that remains dispersed in the medium, which dramatically drops when the solutions are centrifuged after the application of the ultrasonic probe.

3.4. Study of the Stern-Volmer relationship for diluted dispersions of GO in tannic acid.

The fluorescence data of the Stern-Volmer plots discussed above correspond to dispersions prepared independently. Another study was carried out by diluting the initial dispersions (prepared without or with centrifugation) with water or with TA.

3.4.1. Stern-Volmer relationship for riboflavin fluorescence in the presence of GO dispersions in tannic acid, [GO]/[TA] ratio constant.

The initial concentrations of GO in the dispersions in TA 500 mg L^{-1} and 2000 mg L^{-1} were 10, 20, 30 mg L^{-1} and 10, 20 mg L^{-1}, respectively. These were diluted with water to obtain, in the GO dispersions in TA, different concentrations of both components keeping the [GO]/[TA] ratio constant.

Fig. 9 shows the variation of F_0/F *vs* [GO] for aqueous (Fig. 9a, Section 3.2.2.) and TA (Fig. 9b and 9c) dispersions of GO, without or with centrifugation. The presence of TA causes a decrease in riboflavin fluorescence with increasing GO concentration, particularly for the higher TA concentration, 2000 mg L^{-1}.

For dispersions in the absence of TA without centrifugation (Fig. 9a), an exponential trend is observed that may be due to the coexistence of different fluorescence deactivation processes, as mentioned in section 3.2.2. Conversely, in the presence of TA, for the non-centrifuged dispersions, a linear relationship is found for a wide range of low concentrations (Fig. 9b). Regarding the centrifuged dispersions, the observed behavior is different from that found in the absence of TA. The higher the TA concentration, the higher the slope of the linear range, which increases from almost

Table 2
Multiple regression for F_0/F data (95% confidence) as a function of GO and TA concentrations. Quenching constant for GO (K_{GO}) and for TA (K_{TA}).

$F_0/F = C + K_{GO}$ [GO] + K_{TA} [TA]					
NON-CENTRIFUGED					
R^2 = 93.5%	**Value**	**Standard deviation**	**Confidence Interval**		**P-value**
Constant (C)	0.7	0.2	0.3	1.2	0.0042
K_{GO}, L mg $^{-1}$	0.087	0.007	0.071	0.103	0.0000
K_{TA}, L mg $^{-1}$	0.0007	0.0001	0.0004	0.0010	0.0001
CENTRIFUGED					
R^2 = 98.5%	**Value**	**Standard deviation**	**Confidence Interval**		**P-value**
Constant (C)	0.98	0.04	0.90	1.05	0.0000
K_{GO}, L mg $^{-1}$	0.005	0.001	0.003	0.008	0.0014
K_{TA}, L mg $^{-1}$	0.00060	0.00002	0.00055	0.00064	0.0000

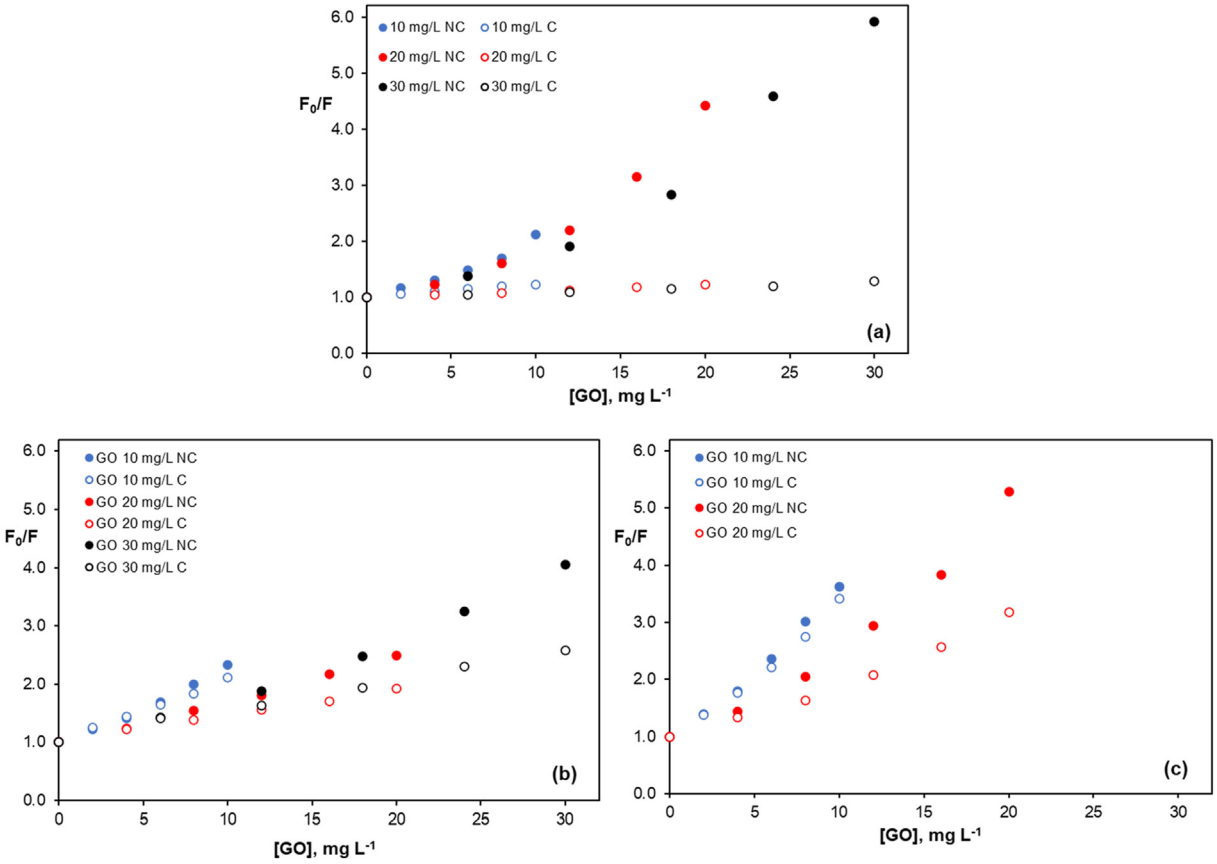

Fig. 9. Stern-Volmer plot (F_0/F *vs* [GO]) for riboflavin 0.6 mg L^{-1} in dispersions of GO in water (a), see Section 3.2.2., and TA 500 mg L^{-1} (b), 2000 mg L^{-1} (c) with constant [GO]/[TA] ratio, for centrifuged (C) and non-centrifuged (NC) dispersions. $\lambda_{exc}/\lambda_{em}$ = 455/520 nm. pH = 7.1.

0 (no change in the riboflavin fluorescence) in the absence of TA to a higher value for a TA concentration of 2000 mg L^{-1}. This corroborates the contribution of TA to improve the GO exfoliation in the centrifuged dispersions.

Fig. 10 shows the effect of TA concentration on riboflavin fluorescence quenching in the GO dispersions. Nonetheless, the differences between centrifuged and non-centrifuged dispersions are less significant versus TA concentration.

To study simultaneously the influence of both quenchers, GO and TA, multiple regression analysis of the data was performed for both centrifuged and non-centrifuged dispersions, and the results are shown in Table 3. The relationship between the experimental F_0/F data and the corresponding values predicted by the theoretical model are shown in **Figure S4** in the supplementary material.

As can be observed in Table 3, the quenching constant K_{GO} is higher for the non-centrifuged dispersions than for the centrifuged ones, leading to constant values very similar to those found for the non-diluted dispersions (Table 2). Regarding the centrifuged dispersions, the fit to the equation is poorer (70.2%), but the K_{TA} value is also similar to that obtained for the non-diluted dispersions. The P-value for the variable [GO] is higher than 0.05 and thus, the influence of GO in the decrease of the riboflavin fluorescence is not significant. This fact implies that the quenching is due to the presence of TA in the medium. It is very important to note that the maximum amount of GO that was initially dispersed and remains in the bulk of the dispersion depends crucially on the application or not of a centrifugation step. In addition, when the fluorescence of riboflavin in the dispersions is measured, the centrifuged dispersions show a lower correlation with GO and TA concentrations for the diluted dispersions than for the dispersions prepared without dilution.

Nonetheless, the K_{TA} values hardly change (0.0006 ± 0.0002 to 0.00085 ± 0.00007), meaning that the interaction of riboflavin with

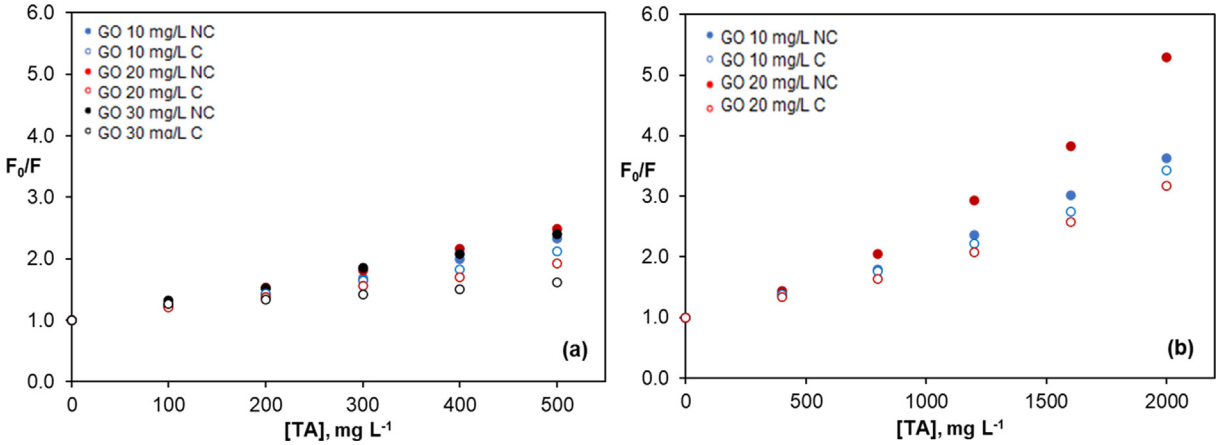

Fig. 10. Stern-Volmer plot (F_0/F *vs* [TA]) for riboflavin 0.6 mg L^{-1} in dispersions of GO in TA 500 mg L^{-1} (a) and 2000 mg L^{-1} (b) with constant [GO]/[TA] ratio, for centrifuged (C) and non-centrifuged (NC) dispersions. $\lambda_{exc}/\lambda_{em}$ = 455/520 nm. pH = 7.1.

Table 3
Multiple regression for F_0/F data (95% confidence) as a function of GO and TA concentrations for diluted dispersions with water (constant [GO]/[TA] ratio). Quenching constant for GO (K_{GO}) and for TA (K_{TA}).

$F_0/F = C + K_{GO}$ [GO] + K_{TA} [TA]					
NON-CENTRIFUGED					
R^2 = 93.4%	**Value**	**Standard deviation**	**Confidence Interval**		**P-value**
Constant (C)	0.85	0.08	0.69	1.02	0.0000
K_{GO}, L mg $^{-1}$	0.082	0.004	0.073	0.091	0.0000
K_{TA}, L mg $^{-1}$	0.00085	0.00007	0.00070	0.00100	0.0000
CENTRIFUGED					
R^2 = 70.2%	**Value**	**Standard deviation**	**Confidence Interval**		**P-value**
Constant (C)	1.18	0.08	1.01	1.35	0.0000
K_{GO}, L mg $^{-1}$	0.006	0.005	−0.003	0.015	0.1910
K_{TA}, L mg $^{-1}$	0.00070	0.00007	0.00055	0.00085	0.0000

TA in the bulk dispersion is constant. Besides, is the same to that obtained in the absence of GO and does not depend on the centrifugation. Therefore, the quenching produced by TA in the fluorescence of riboflavin is independent of the GO concentration and the centrifugation step.

3.4.2. Study of the Stern-Volmer relationship for GO dispersions in tannic acid, [GO]/[TA] ratio variable.

The initial concentrations of GO in the dispersions in TA 500 and 2000 mg L^{-1} were 10, 20, 30 mg L^{-1} and 10, 20 mg L^{-1}, respectively. These were diluted with TA to obtain different GO concentrations albeit keeping the TA concentration constant, thus the [GO]/[TA] ratio was variable.

Fig. 11 shows the Stern-Volmer plot for dispersions that were diluted with the same concentration of TA used in the preparation of the dispersion and the corresponding quenching parameters are collected in Table 4.

Since the TA concentration is constant, this parameter cannot be the responsible for the changes found in the interaction of riboflavin with GO, thus it is easier to assess the interaction between them. In this case, the linear fit to Stern-Volmer relation only depends on the riboflavin-GO interaction, while it is independent of the proportional amount of GO from the initial concentration dispersed in each bulk dispersion.

As can be observed in Fig. 11, the Stern-Volmer plot is linear in all cases, and the quenching produced by GO on the fluorescence of riboflavin is higher again in the solutions prepared from non-centrifuged dispersions than in those prepared from centrifuged ones.

Nevertheless, the comparison of the results plotted in Fig. 10 (constant [G]/[AT] ratio) with those plotted in Fig. 11 (constant [TA]) reveals that the quenching produced by GO on the fluorescence of riboflavin is significantly lower than that caused by TA. The quenching constants obtained in dispersions with 500 mg L^{-1} AT and 2000 mg L^{-1} are fairly similar, showing lower values for the centrifuged dispersions with the higher percentages of GO with respect to TA in the initial solution.

The centrifuged dispersions have a low concentration of GO in the bulk solution and when the F_0/F ratio is calculated using the fluorescence of riboflavin in TA solution as F_0 value, only a small change in the riboflavin fluorescence is found due to the very low GO concentration. In the non-centrifuged dispersions, higher quenching induced by GO is detected, pointing towards a high concentration of GO in the bulk dispersion.

The K_{GO} values obtained are systematically lower for the centrifuged dispersions; besides, they are lower for dispersions with a constant TA concentration compared to the dispersions diluted with water ([GO]/[TA] constant). This corroborates that when both GO and TA are present, TA is the main contributor to the quenching effect, hence the effect of GO is lower and therefore the quenching constants are also lower.

3.5. Comparison between tannic acid dispersing efficiency and the interaction of riboflavin with graphene and graphene oxide

In a previous work of our research group [34], the dispersion of G in the presence of TA was investigated. In that study, all the dispersions were subjected to centrifugation, since G is hydrophobic in nature, hence large agglomerates are formed if its dispersions are not centrifuged. A quenching effect of riboflavin fluorescence by G was also observed, which has been compared with that found in this work by GO centrifuged dispersions.

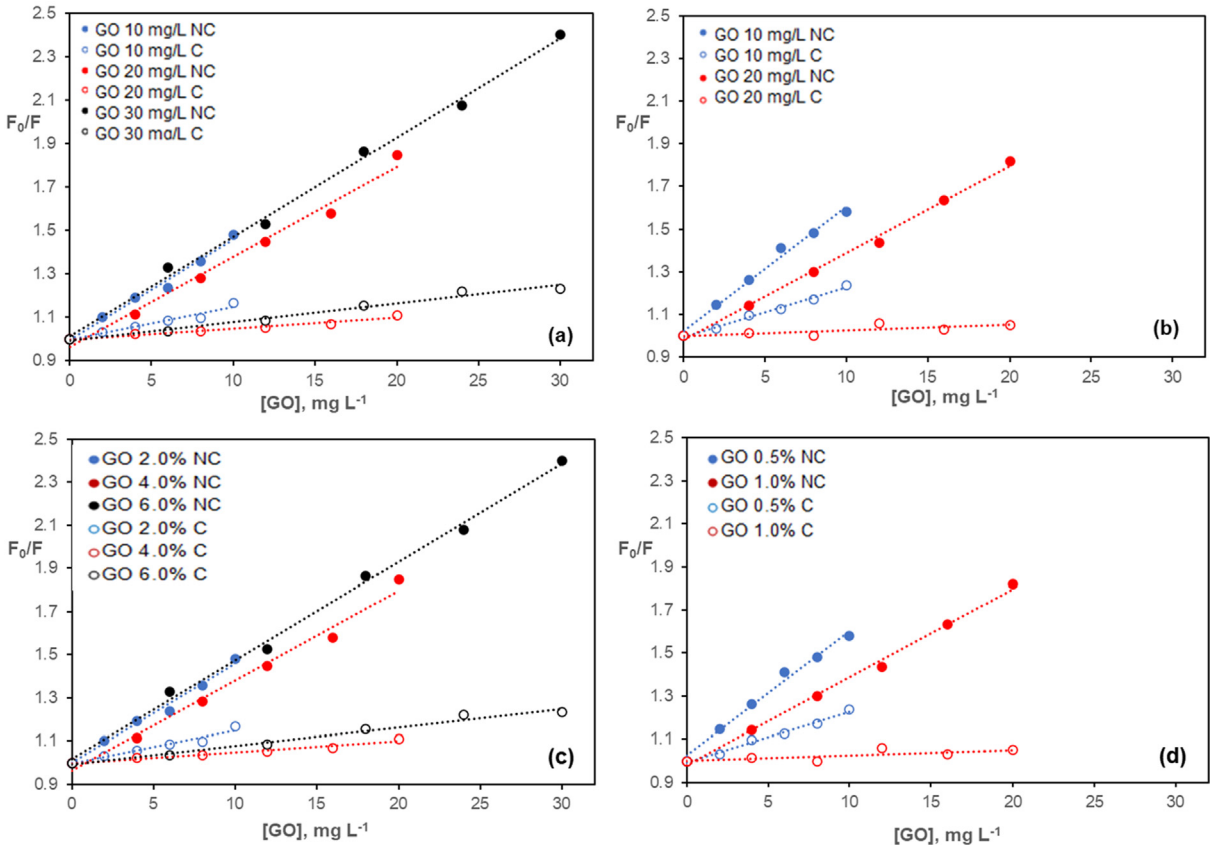

Fig. 11. Stern-Volmer plot for riboflavin 0.6 mg L^{-1} in dispersions of GO in a constant [TA] concentration of 500 mg L^{-1} (a),(c) and 2000 mg L^{-1} (b),(d), centrifuged (C) and non-centrifuged (NC). $\lambda_{exc}/\lambda_{em}$ = 455/520 nm.

Table 4
Parameters obtained by fitting the experimental results to the Stern-Volmer equation (least-square fit procedure), for a constant [TA].

500 mg L^{-1} TA						
GO, wt%	**2.0 NC**	**4.0 NC**	**6.0 NC**	**2.0 C**	**4.0 C**	**6.0 C**
[GO], mg L^{-1}	**0 – 10**	**0–20**	**0–30**	**0–10**	**0–20**	**0–30**
Intercept	1.003 ± 0.009	0.99 ± 0.01	1.02 ± 0.03	0.995 ± 0.006	1.003 ± 0.003	0.995 ± 0.008
K, L mg^{-1}	0.046 ± 0.001	0.037 ± 0.001	0.046 ± 0.001	0.016 ± 0.001	0.0042 ± 0.0003	0.0081 ± 0.0005
r	0.999	0.998	0.998	0.994	0.993	0.995
2000 mg L^{-1} TA						
GO, wt%	**0.5 NC**	**1.0 NC**	**0.5 C**	**1.0 C**		
[GO], mg L^{-1}	**0–10**	**0–20**	**0–10**	**0–20**		
Intercept	1.02 ± 0.01	0.98 ± 0.02	0.994 ± 0.008	1.002 ± 0.005	NC: Non-Centrifuged	
K, L mg^{-1}	0.057 ± 0.002	0.041 ± 0.001	0.023 ± 0.001	0.0022 ± 0.0004	C: Centrifuged	
r	0.998	0.998	0.994	0.970		

Fig. 12 compares the quenching constants obtained for G (taken from [34]) and GO centrifuged dispersions with the same concentration of nanomaterial (N) and TA.

The values were calculated taking the nanomaterial concentration as the only variable, without taking in account the TA contribution. For identical conditions, the values obtained for G are higher than those for GO.

As the nanomaterial percentage increases, K values decrease, and this drop is stronger for dispersions with a constant TA concentration. In these dispersions, only the interaction between riboflavin and the nanomaterial is taken into account, hence K values are much lower than when considering the interaction of riboflavin with both GO and TA.

3.6. TEM analysis of the GO dispersions

The quality of GO dispersions in water and TA was further assessed by TEM, and representative images of 10 mg L^{-1} GO dispersion in water and in 2000 mg L^{-1} TA, both centrifuged and non-centrifuged, are compared in Fig. 13.

A set of stacked and curled sheets can be observed in the sample comprising only GO. When TA is added, the sheets appear more disentangled and smoother, due to the ability of TA to disperse the GO sheets and keep them stable. In these cases, traces of TA are observed between sheets that are arranged in the form of drops or darker spots. On the other hand, when a sample comprising both GO and TA was subjected to centrifugation, only a few thin mono-

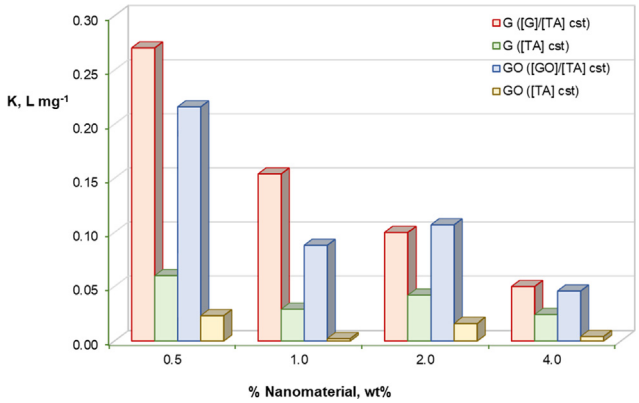

Fig. 12. Quenching constants (K) for GO and G centrifuged dispersions with an initial TA concentration of 500 mg L^{-1} (2.0 and 4.0 wt%) and 2000 mg L^{-1} (0.5 and 1.0 wt%) with a constant ratio [N]/[TA] and a constant [TA]. $\lambda_{exc}/\lambda_{em}$ = 455/520 nm.

layers were isolated, due to the combined effect of TA that stabilized the sheets and the centrifugation step that removed the aggregated and larger nanosheets, which are heavier. Therefore, the centrifugation should be avoided in order to obtain a good dispersion with a high amount of GO in the bulk solution. This separation step removes a large quantity of GO that is not agglomerated in the dispersion, thus decreasing significantly the riboflavin-GO interaction.

As can be observed in Fig. 14, when the dispersions with different GO concentrations obtained without centrifugation were analysed by TEM, a few layers of GO were found, showing structures very similar to those observed in the centrifuged dispersions.

Overall, TEM analysis corroborates the effectiveness of TA as dispersant agent for GO in aqueous solutions and demonstrate that the level of exfoliation attained depends only slightly on the GO or TA concentration, albeit it is conditioned by the application of a centrifugation stage.

4. Conclusions

An important quenching of riboflavin fluorescence has been observed in the presence of TA, which has been found to be independent of the centrifugation step, but dependent on the TA concentration, being very significant at a concentration of 2000 mg L^{-1}. The strong interaction of riboflavin with TA via structure modification by H-bonding and π-π interactions between the isoalloxazine rings of the vitamin and the phenolic rings of TA, is responsible of the quenching process.

GO aqueous dispersions, without any additional dispersant, also induce a quenching of riboflavin fluorescence, which is strongly influenced by the centrifugation step. This quenching is very pronounced in the absence of centrifugation, since after centrifugation the GO aggregates settle at the bottom of the tube and only a few sheets remain dispersed in the water medium.

Experimental data have been fitted to the Stern-Volmer equation in order to obtain the values of the quenching constants. The data for the non-centrifuged dispersions only follows a linear relationship over a small range of GO concentrations, showing an exponential trend, indicative of the co-existence of the two types of quenching mechanisms, dynamic and static. However, for the centrifuged dispersions the data fit a straight line in the whole studied range, according to the Stern-Volmer model. In this case, the values of the quenching constant decrease with increasing

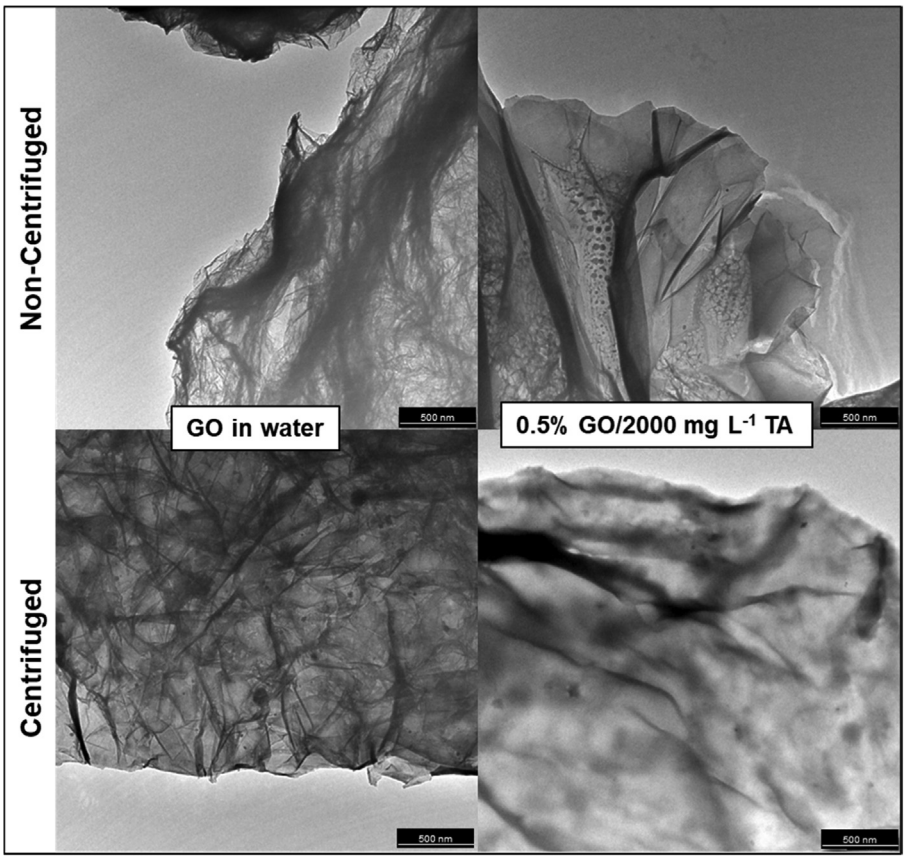

Fig. 13. TEM micrographs of 10 mg L^{-1} GO dispersion in water and in 2000 mg L^{-1} TA, non-centrifuged and centrifuged. Magnification 16000x.

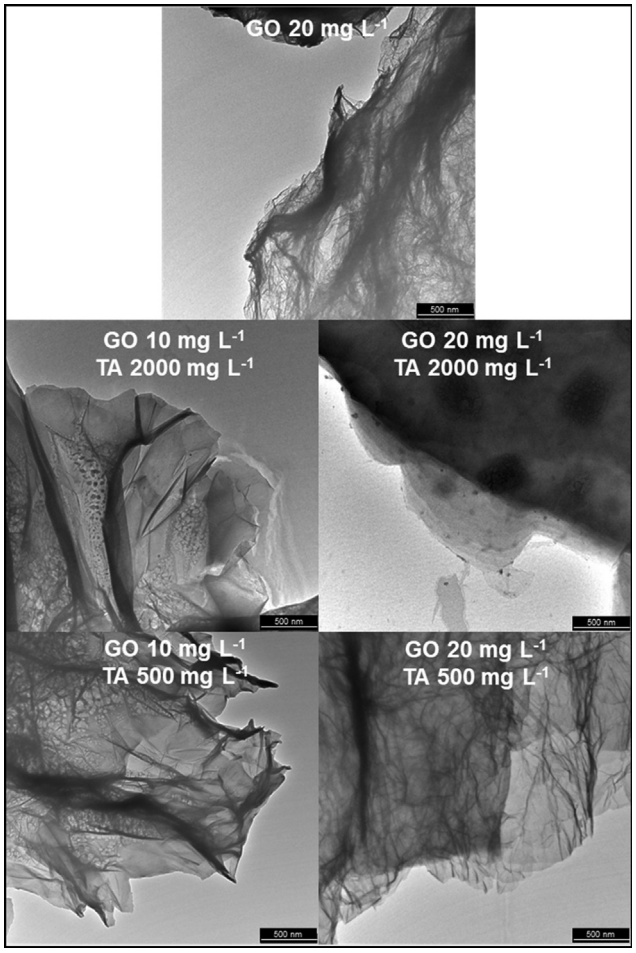

Fig. 14. TEM micrographs of non-centrifuged GO dispersions: 10 mg L^{-1} GO in water and 10 and 20 mg L^{-1} GO in 500 and 2000 mg L^{-1} TA. Magnification 16000x.

GO concentration, indicative of a poor GO dispersion using water as the only dispersant.

The use of a bioactive molecule, TA, as a dispersing agent for GO has been tested. TEM analysis corroborates its high effectiveness as dispersant agent in aqueous solutions and demonstrates that the level of GO exfoliation attained is conditioned by the application of a centrifugation stage.

GO dispersions in TA, prepared either *in situ* or by dilution ([GO]/[TA] constant) produce an important quenching of riboflavin fluorescence. Data obtained in the presence of TA or the GO dispersions in TA have been adjusted by means of a multiple regression analysis, in order to evaluate simultaneously the effect of GO and TA on the dispersions. Results indicate that TA is the main responsible for the quenching process.

Regarding GO dispersions at a constant [TA], GO concentration is the only variable. In this case, it is possible to apply the Stern-Volmer model over a wider range of GO concentrations. The values of the quenching constants for dispersions at a constant [GO]/[TA] ratio are of the same order of magnitude to those obtained by multiple regression analysis. These results demonstrate the usefulness of the multiple regression method for calculating quenching constants when there is more than one quencher in the medium. In addition, they corroborate that the presence of TA is the major responsible for the quenching of fluorescence of riboflavin.

Overall, it is found that the use of TA as an environmentally friendly dispersant agent instead of organic solvents or synthetic surfactants leads to high-quality carbon nanomaterial dispersions in water, which is interesting in the search for more sustainable and greener processes.

CRediT authorship contribution statement

Carlos Sainz-Urruela: Investigation. **Soledad Vera-López:** Writing – review & editing. **Ana María Díez-Pascual:** Writing – review & editing. **María Paz San Andrés:** Methodology, Writing – original draft, Supervision.

Declaration of Competing Interest

The authors declare that they have no known competing financial interests or personal relationships that could have appeared to influence the work reported in this paper.

Acknowledgements

The authors wish to thank the Spanish Ministry of Science and Innovation and Universities (MICIU) for funding the work (Project PGC2018-093375-B-I00).

Appendix A. Supplementary data

Supplementary data to this article can be found online at https://doi.org/10.1016/j.saa.2022.121302.

References

[1] C. Soldano, A. Mahmood, E. Dujardin, Production, properties and potential of graphene, Carbon 48 (2010) 2127–2150, https://doi.org/10.1016/j.carbon.2010.01.058.
[2] K.S. Novoselov, A.K. Geim, S.V. Morozov, D. Jiang, Y. Zhang, S.V. Dubonos, I.V. Grigorieva, A.A. Firsov, Electric field effect in atomically thin carbon films, Science 306 (2004) 666–669, https://doi.org/10.1126/science.1102896.
[3] A.A. Balandin, S. Ghosh, W. Bao, I. Calizo, D. Teweldebrhan, F. Miao, C.N. Lau, Superior thermal conductivity of single-layer graphene, Nano Lett. 8 (3) (2008) 902–907, https://doi.org/10.1021/nl0731872.
[4] A.M. Díez-Pascual, M.A. Gómez-Fatou, F. Ania, A. Flores, Nanoindentation in Polymer Nanocomposites, Prog. Mater. Sci. 67 (2015) 1–94, https://doi.org/10.1016/j.pmatsci.2014.06.002.
[5] M.K. Kavitha, M. Jaiswa, Graphene: A review of optical properties and photonic applications, Asian J. Physics. 25 (7) (2016) 809–831.
[6] A.M. Diez-Pascual, A.L. Diez-Vicente, Poly(propylene fumarate)/polyethylene glycol-modified graphene oxide nanocomposites for tissue engineering, ACS Appl. Mater. Interface. 8 (2016) 7902–17914, https://doi.org/10.1021/acsami.6b05635.
[7] H. Salavagione, A.M. Díez-Pascual, E. Lázaro, S. Vera, M. Gomez-Fatou, Chemical sensors based on polymer composites with carbon nanotubes and G. The role of the polymer, J. Mater. Chem. 2 (2014) 14289–14328, https://doi.org/10.1039/C4TA02159B.
[8] W.S. Hummers, R.E. Offeman, Preparation of Graphitic Oxide, J. Am. Chem. Soc. 80 (6) (1958) 1339.
[9] G.I. Titelman, V. Gelman, S. Bron, R.L. Khalfin, Y. Cohen, H. Bianco-Peled, Characteristics and microstructure of aqueous colloidal dispersions of graphite oxide, Carbon 43 (2005) 641–649, https://doi.org/10.1016/j.carbon.2004.10.035.
[10] D.R. Dreyer, S. Park, C.W. Bielawski, R.S. Ruoff, The Chemistry of Graphene Oxide, Chem. Soc. Rev. 39 (2010) 228–240, https://doi.org/10.1039/B917103G.
[11] A.M. Díez-Pascual, C. Sainz-Urruela, C. Vallés, S. Vera-López, M.P. San Andrés, Tailorable Synthesis of Highly Oxidized Graphene Oxides via an Environmentally-Friendly Electrochemical Process, Nanomaterials. 10 (2020) 239, https://doi.org/10.3390/nano10020239.
[12] C. Sainz-Urruela, S. Vera-López, M.P. San Andrés, A.M. Díez-Pascual, Graphene Oxides Derivatives Prepared by an Electrochemical Approach: Correlation between Structure and Properties, Nanomaterials. 10 (2020) 2532, https://doi.org/10.3390/nano10122532.
[13] S. Kamiloglu, M. Tomas, T. Ozdal, P. Yolci-Omeroglu, E. Capanoglu, Bioactive component analysis. In "Innovative Food Analysis", Charis Galanakis (Ed), Elsevier Science Publishing Co Inc. (2020) Chapter 2, pp. 41-65.
[14] C. Sainz-Urruela, S. Vera-López, M.P. San Andrés, A.M. Díez-Pascual, Graphene-Based Sensors for the Detection of Bioactive Compounds: A Review, Int. J. Mol. Sci. 22 (2021) 3316, https://doi.org/10.3390/ijms22073316.
[15] P. Buzzini, P. Arapitsas, M. Goretti, E. Branda, B. Turchetti, P. Pinelli, F. Leri, A. Romani, Antimicrobial and antiviral activity of hydrolysable tannins, Mini-Rev. Med. Chem. 8 (2008) 1179–1187, https://doi.org/10.2174/138955708786140990.

[16] E. Tomaszewska, P. Dobrowolski, A. Winiarska-Mieczan, M. Kwiecien, A. Tomczyk, S. Muszynski, The effect of tannic acid on the bone tissue of adult male Wistar rats exposed to cadmium and lead, Exp. Toxicol. Pathol. 69 (69) (2017) 131–141, https://doi.org/10.1016/j.etp.2016.12.003.
[17] S. Lau, J. Wahn, G. Schulz, C. Sommerfeld, U. Wahn, Placebo-controlled study of the mite allergen-reducing effect of tannic acid plus benzyl benzoate on carpets in homes of children with house dust mite sensitization and asthma, Pediatric Allergy and Immunology. 13 (2002) 31–36, https://doi.org/10.1034/j.1399-3038.2002.00073.x.
[18] S. Zhao, S. Xie, Z. Zhao, J. Zhang, L. Li, Z. Xin, Green and high-efficiency production of graphene by tannic acid-assisted exfoliation of graphite in water, ACS Sustain. Chem. Eng. 6 (2018) 7652–7661, https://doi.org/10.1021/acssuschemeng.8b00497.
[19] R.S. Rivlin. Riboflavin. In: "Encyclopedia of Dietary Supplements." P.M. Coates, J.M. Betz, M.R. Blackman et al. (eds.) 2nd ed. London and New York: Informa Healthcare. (2010) 691-699.
[20] R. Mateos, S. Vera, M. Valiente, A.M. Díez-Pascual, M.P. San Andrés, Comparison of Anionic, Cationic and Nonionic Surfactants as Dispersing Agents for Graphene Based on the Fluorescence of Riboflavin, Nanomaterials. 7 (11) (2017) 403, https://doi.org/10.3390/nano7110403.
[21] J.R. Lakowicz, Principles of Fluorescence Spectroscopy, Springer US, Boston, MA, 2006.
[22] J.B. Birks, Photophysics of aromatic molecules, Wiley-Interscience, London, 1970.
[23] J. Keizer, Diffusion effects on rapid bimolecular chemical reactions, Chem. Rev. 87 (1987) 167–180, https://doi.org/10.1021/cr00077a009.
[24] S. Vera-López, P. Martínez, M.P. San Andrés, A.M. Díez-Pascual, M. Valiente, Study of graphene dispersions in sodium dodecylsulfate by steady-state fluorescence of pyrene, J. Colloid Int. Sci. 514 (2018) 415–424, https://doi.org/10.1016/j.jcis.2017.12.052.
[25] R. Mateos, A. Garcia-Zafra, S. Vera-López, M.P. San Andrés, A.M. Díez-Pascual, Effect of Graphene Flakes Modified by Dispersion in Surfactant Solutions on the Fluorescence Behaviour of Pyridoxine, Materials. 11 (2018) 881–902, https://doi.org/10.3390/ma11060888.
[26] J.I. Paredes, S. Villar-Rodil, Biomolecule-assisted exfoliation and dispersion of graphene and other two-dimensional materials: a review of recent progress and applications, Nanoscale. 8 (2016) 15389–15413, https://doi.org/10.1039/C6NR02039A.
[27] P. Laaksonen, M. Kainlauri, T. Laaksonen, A. Shchepetov, H. Jiang, J. Ahopelto, M.B. Linder, Interfacial engineering by proteins: exfoliation and functionalization of graphene by hydrophobins, Angew. Chem. Int. Ed. 49 (2010) 4946–4949, https://doi.org/10.1002/anie.201001806.
[28] M. Pykal, K. Safárová, K.M. Sisková, P. Jurecka, A.B. Bourlinos, R. Zboril, M. Otyepka, Lipid Enhanced Exfoliation for Production of Graphene Nanosheets, J. Phys. Chem. C. 117 (2013) 11800–11803, https://doi.org/10.1021/jp401277g.
[29] A.P.A. Raju, S.C. Offerman, P. Gorgojo, C. Valles, E.V. Bichenkova, H.S. Aojula, A. Vijayraghavan, R.J. Young, K.S. Novoselov, I.A. Kinloch, D.J. Clarke, Dispersal of pristine graphene for biological studies, RSC Adv. 6 (2016) 69551–69559, https://doi.org/10.1039/C6RA12195K.
[30] S. Gurunathan, J.W. Jan, E.S. Kim, J.Y. Park, J.H. Kim, Reduction of graphene oxide by resveratrol: A novel and simple biological method for the synthesis of an effective anticancer nanotherapeutic molecule, Int. J. Nanomed. 10 (2015) 2951–2969, https://doi.org/10.2147/IJN.S79879.
[31] A.H. Abdullah, Z. Ismail, A.S.Z. Abidin, K. Yusoh, Green sonochemical synthesis of few-layer graphene in instant coffee, Mater. Chem. Phys. 222 (2019) 11–19, https://doi.org/10.1016/j.matchemphys.2018.09.085.
[32] Y. Wang, Z. Shi, J. Yin, Facile synthesis of soluble graphene via a green reduction of graphene oxide in tea solution and its biocomposites, ACS Appl. Mater. Interfaces. 3 (2011) 1127–1133, https://doi.org/10.1021/am1012613.
[33] M.J.Y. Tai, W.W. Liu, C.S. Khe, N.M.S. Hidayah, Y.P. Teoh, C.H. Voon, H.C. Lee, P. Y.P. Adelyn, Green synthesis of reduced graphene oxide using green tea extract, AIP Conference Proceedings. 2045 (2018), https://doi.org/10.1063/1.5080845 020032.
[34] M.P. San Andrés, M. Baños-Cabrera, L. Gutiérrez-Fernández, A.M. Díez-Pascual, S. Vera-López, Fluorescence Study of Riboflavin Interactions with Graphene Dispersed in Bioactive Tannic Acid, Int. J. Mol. Sci. 22 (2021) 5270, https://doi.org/10.3390/ijms22105270.
[35] K. Grigoryan, L. Sargsyan, T. Burkholz, C. Jacob, Fluorescence characterization of human hemoglobin binding with tannic acid, Chem. J. Armenia 67 (2014) 181–187.